

SU(N) Quantum Spin Model with Weak and Strong First-Order Néel to Valence-Bond Solid Transitions

Ryan Flynn* and Anders W. Sandvik†

Department of Physics, Boston University, 590 Commonwealth Avenue, Boston, Massachusetts 02215, USA

(Dated: March 18, 2026)

We introduce an SU(N) symmetric two-dimensional quantum spin model, the X - Q model, which hosts a ground state transition between Néel antiferromagnetic and spontaneously dimerized states. The Q terms are products of two adjacent singlet projectors on nearest-neighbor sites, as in the often studied J - Q model (where J is the Heisenberg exchange), while the X terms are products of two permutation operators on second-neighbor sites. Quantum Monte Carlo simulations reveal close proximity to a deconfined quantum critical point for $N = 2$, as in the J - Q model. However, for $N > 2$ the transition becomes strongly first-order, contrary to conventional expectations that increasing N should weaken discontinuities. We attribute this behavior to the inability of the X term, which dominates at the transition for large N , to induce U(1) fluctuations of the dimer pattern. These results provide insights into the microscopic interactions that support deconfined criticality.

Two-dimensional (2D) quantum antiferromagnets on the square lattice provide a central platform for the study of strongly correlated quantum matter [1–4]. Their ground state is typically characterized by Néel antiferromagnetic (AFM) order, and understanding how this order is destabilized has been a long-standing problem [5–11] since the discovery of high-temperature superconductivity emerging in the cuprates upon doping [12]. Another case, the transition from an AFM state to a spontaneously dimerized ground state (the valence-bond solid, VBS) [13–19], is of fundamental interest in its own right and also has potential intersections with the still unresolved high- T_c problem [20]. Following suggestive numerical findings [21–23], the theory of deconfined quantum criticality (DQC) [24–27] posits that such a transition can be continuous, involving fractionalized excitations, an emergent gauge field, and enhanced symmetries. Such transitions lie beyond the conventional Landau–Ginzburg–Wilson paradigm, where a transition between ordered states breaking unrelated symmetries is generically of first-order.

Early quantum Monte Carlo (QMC) results for the 2D J - Q spin models hosting the AFM–VBS transition confirmed the key prediction of emergent U(1) symmetry of the microscopically \mathbb{Z}_4 symmetric VBS order parameter near criticality [28–31], reflecting “dangerous irrelevance” of the lattice anisotropy; a well-known phenomenon in classical clock models [32–34]. Subsequent studies of SU(N) models [31, 35–38] found quantitative agreement with large- N field-theoretic predictions that the AFM–VBS transition is described by the non-compact CP^{N-1} model [25, 39].

Despite this convergence of results, there is continued disagreement on the nature of the transition for small N . The SU(2) lattice models do not exhibit clean criticality, instead showing finite-size effects that have been interpreted either as weak first-order transitions [29, 40–45] or anomalous corrections inherent to DQC [46–48]. In one scenario, the inability to reach the critical point

exactly is a fundamental aspect of SU(2) DQC—its description by a complex conformal field theory (CFT) with an unphysical fixed point [49–51]. A competing view is that DQC arises from a multicritical point at the tip of the gapless spin liquid that has been observed in numerics between AFM and VBS phases [52–60] and for which various field theories have been proposed [61, 62]. These spin liquids are out of reach of sign-problem-free simulations and the multicritical point may therefore also be difficult (or impossible) to reach. The most recent large-scale QMC simulations of the J - Q model [63] nevertheless demonstrate very close proximity to a critical point with emergent SO(5) symmetry [47] and good agreement with exponents from related CFT calculations [64].

These developments and the persistent controversy regarding $N = 2$ (and other small N) [51, 65–67] motivate the exploration of alternative lattice realizations that could potentially be tuned even closer to the proposed multicritical DQC point. Here we introduce the SU(N) X - Q model, a sign-problem-free Hamiltonian that, like the J - Q model, exhibits a direct AFM–VBS transition but differs in the operator that stabilizes the AFM state; the X term consists of permutation operators on second-neighbor sites instead of the standard exchange J . This model supports an AFM–VBS transition at arbitrary N , whereas the $N > 4$ J - Q models only do if other interactions are added [19, 37]. Contrary to expectations that increasing N favors critical behavior, we find the opposite trend: while the transition is only weakly first-order for SU(2), it becomes increasingly discontinuous for larger N .

We attribute this unexpected behavior to the absence of emergent U(1) symmetry in the VBS order parameter for large N (in practice all $N > 2$). Unlike the singlet projectors of the J - Q model, the X permutation does not induce resonances between local VBS orientations, thus not enabling global rotations of the order parameter. We also explain why the large- N X - Q model does not flow to the same non-compact CP^{N-1} continuum description

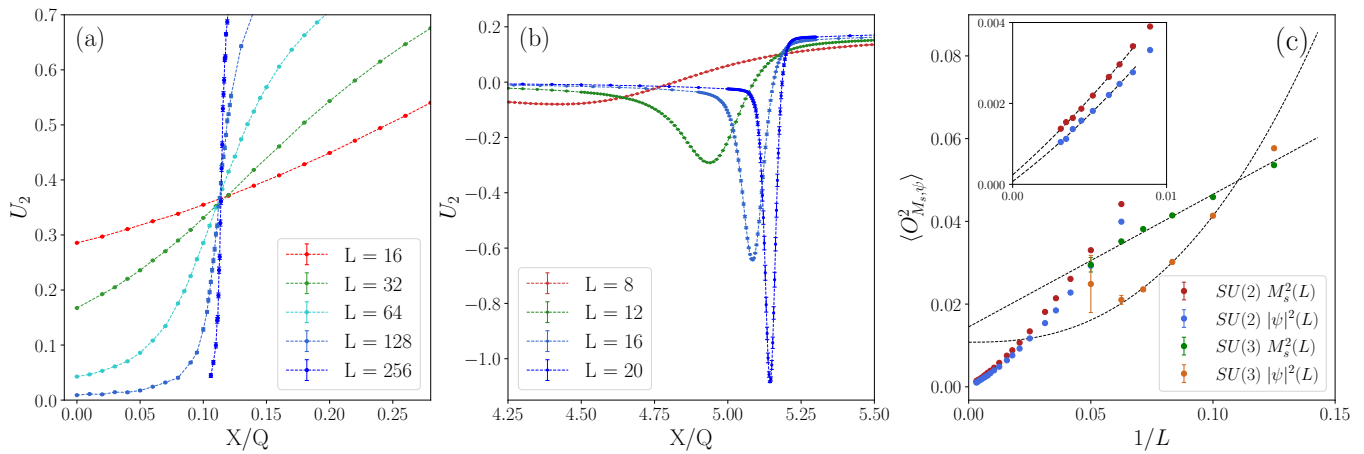


FIG. 1. Binder cumulant for (a) SU(2) systems with $L = 16$ – 256 and (b) SU(3) systems with $L = 8$ – 20 . In (a) the fitted curves cross at the near-critical point $(X/Q)_c \approx 0.115$ while in (b) the negative peak flows to a clearly first-order transition at $(X/Q)_c \approx 5.2$. (c) Extrapolations of the order parameters M_s^2 and $|\psi|^2$ at the transition point [defined by cumulant crossings for SU(2) and cumulant minima for SU(3)], with the non-zero $L \rightarrow \infty$ values demonstrating phase coexistence in both models. Polynomial fits were used for all order parameters, except $|\psi|^2$ for SU(3), where the manifestly discrete symmetry breaking implies exponential convergence. The inset in (c) zooms in on the large- L SU(2) data.

[24, 25, 39] as the extended J - Q models [37, 38], but instead freezes into a trivial columnar VBS state at the transition.

Model and Methods.—We define the SU(N) square-lattice X - Q model in the standard way [15, 16] in which the two sublattices carry the fundamental and conjugate SU(N) representations, corresponding to Young tableaux with one box and a column of $N - 1$ boxes respectively. This structure allows nearest neighbors to form SU(N) singlets of N “colors”. The Hamiltonian is

$$H = -\frac{X}{N^2} \sum_{\langle\langle ijkl \rangle\rangle} \Pi_{il} \Pi_{jk} - \frac{Q}{N^2} \sum_{\langle ijkl \rangle} P_{ij} P_{kl}, \quad (1)$$

where $\langle ijkl \rangle$ indicates that P_{ij} (singlet projectors) act on nearest-neighbor bonds of 2×2 plaquettes and $\langle\langle ijkl \rangle\rangle$ that Π_{ij} (permutation operators) act on same-sublattice next-nearest-neighbor bonds on periodic $L \times L$ lattices. These operators can be written in terms of the SU(N) generators T^a as

$$\begin{aligned} \frac{1}{N^2} P_{ij} &= \frac{1}{N^2} - \frac{2}{N} T_i^a T_j^a, \\ \frac{1}{N^2} \Pi_{ij} &= \frac{1}{N^2} + \frac{2}{N} T_i^a T_j^a. \end{aligned} \quad (2)$$

Here the X term permutes colors on the same sublattice, favoring color alignment within each sublattice and stabilizing AFM order. The Q term favors singlet formation on nearest-neighbor bonds and couples the two sublattices, promoting VBS order. The model is sign-problem free for all N and we study it using the stochastic series expansion (SSE) QMC method with operator-loop updates [68, 69] at temperatures sufficiently low ($T \propto L^{-1}$)

to converge to the ground state. For efficient sampling near the strongly first-order $N > 2$ transitions, we employ quantum parallel tempering [70, 71] in the coupling ratio X/Q .

We detect AFM order via the staggered magnetization M_s , while VBS order is probed through its columnar dimer (singlet) pattern. We define these order parameters for SU(N) spins in terms of the $N - 1$ Cartan matrices H^a (listed in the Appendix)

$$m_s^a = \frac{1}{L^2} \sum_i H_{\alpha\alpha}^a n_{i\alpha}, \quad (3a)$$

$$D_\mu^a = \frac{1}{L^2} \sum_x (-1)^\mu H_{\alpha\alpha}^a n_{\mu,\alpha} H_{\alpha\alpha}^a n_{\mu+1,\alpha}, \quad (3b)$$

where $\alpha = 1 \dots N$ is for the N colors, $n_{i,\alpha} = 1$ if color α is on site i , and $\mu = x, y$ denotes x and y orientation. The simulations do not break any symmetries, and we study the squared magnitudes of the order parameters, defining $M_s^2 = \langle \sum_a (m_s^a)^2 \rangle$ and $|\psi|^2 = \langle D_x^2 + D_y^2 \rangle$, with $D_\mu = \sum_a D_\mu^a$. To test for the emergence of U(1) symmetry at the transition, we evaluate the anisotropy $\phi_4 = \langle \cos(4\theta) \rangle$, where θ is the angle corresponding to $\psi = D_x + iD_y$.

For a standard diagnostic of the phase transitions, we define the Binder cumulant for $\mathcal{O} = M_s$ or $\mathcal{O} = \psi$ as

$$U_2 = 1 - \frac{N-1}{N+1} \frac{\langle \mathcal{O}^4 \rangle}{\langle \mathcal{O}^2 \rangle^2}, \quad (4)$$

where the N -dependent prefactor accounts for the multi-component nature of the SU(N) order parameter and reduces to the standard value of $1/3$ for SU(2). This factor ensures $U_2 \rightarrow 0$ in the disordered phase where $\langle \mathcal{O}^2 \rangle \rightarrow 0$

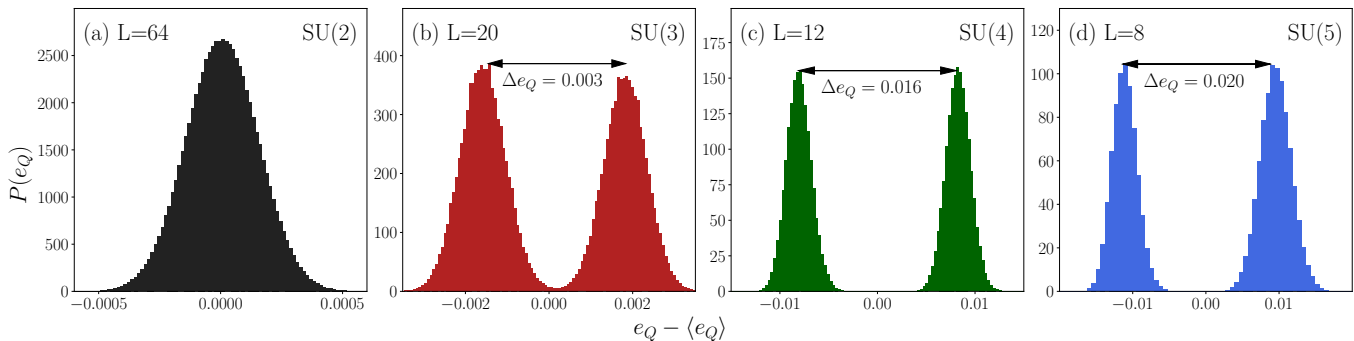


FIG. 2. Q -energy histograms relative to the mean for the $SU(N)$ models. For $N = 2$ in (a), the distribution for $L = 64$ has a single peak, while for $N = 3, 4, 5$ in (b), (c), and (d), respectively, the large peak splitting for the smaller sizes (which are the largest systems studied) signals two-phase coexistence. The indicated peak splitting is almost converged versus L .

when $L \rightarrow \infty$. To more directly probe first-order behavior, we will also use the probability distribution $P(e_Q)$ of the Q part of the energy

Results.—We first discuss the cumulants and order parameters of the $SU(2)$ and $SU(3)$ models. Fig. 1(a) shows U_2 for $SU(2)$ systems up to system size $L = 256$. Fitted curves produce a clear crossing point at $(X/Q)_c \approx 0.115$ and no evidence of a negative dip. In sharp contrast, for $SU(3)$ systems the cumulants in Fig. 1(b) show a dip that deepens in proportion to the space-time volume L^3 , which is a hallmark of a first-order transition [72, 73]. Tunneling between the different phases near the transition quickly becomes intractable, and we have only equilibrated systems up to size $L = 20$. The drifts of the crossings and peaks indicate $(X/Q)_c \approx 5.2$. In Fig. 1(c), $L \rightarrow \infty$ extrapolations of the order parameters show that both take finite values at the transition, thus providing evidence of phase coexistence in these systems. For $SU(2)$, the absence of negative cumulant and the very small extrapolated order parameters puts the transition in the category of very weak first-order transitions, like the J - Q model [63] (with very similar near-critical scaling behavior). The value of the order parameters at the transition is roughly an order of magnitude larger for $SU(3)$, and the sharp negative cumulant peaks suggest that this model (and those for larger N) is far from any critical point.

Fig. 2 shows the Q energy-per-site distribution $P(e_Q)$ at the transition for $N = 2-5$ computed for sizes $L = 64, 20, 12, 8$, respectively. At a quantum phase transition ($T = 0$), the total energy $e = \langle H \rangle / L^2$ is analogous to the free energy at a classical $T > 0$ transition and $P(e)$ is therefore always singly-peaked. The distribution $P(e_Q)$ [or, equivalently, $P(e_X)$] can be used to detect a discontinuity analogously to the internal energy classically. For $N > 2$, the distributions in Fig. 2 are bimodal; a defining signature of phase coexistence at a first-order transition. There is no evidence of bimodality for $SU(2)$, though we do expect the distribution to eventually split for larger

L , given the weak first-order transition demonstrated in Fig. 1. We find that the peak separation Δe_Q increases with N , demonstrating that the transition becomes more strongly first-order, in contrast to the behavior of the $SU(N)$ J - Q models [31, 37].

The strongly first-order transitions in the $SU(N > 2)$ models are associated with the absence of emergent $U(1)$ symmetry; the lattice anisotropy remains relevant. The DQC scenario requires that this anisotropy be “dangerously irrelevant”, i.e., the presumed continuum critical point is stable in the presence of the lattice; the $U(1)$ symmetry will then be emergent for $L \rightarrow \infty$. The relevance of the lattice in the VBS phase is associated with a length scale different from the conventional correlation length, and this length scale is also related to the scale of spinon deconfinement in the neighborhood of a DQC transition [25, 48]. The emergent $U(1)$ symmetry is well known in the case of extended J - Q models for any N [28, 29, 31] and, for the special case of $N = 2$, was later shown to be further enhanced to $SO(5)$, in related 3D classical models [47, 74] and in the J - Q models [63, 75].

The distribution of the VBS order parameter in Fig. 3(a) reflects phase coexistence in the $SU(3)$ case, with only \mathbb{Z}_4 symmetry (spontaneously broken for $L \rightarrow \infty$) of the VBS order. An emergent $U(1)$ symmetry would appear as an increasingly uniform ring $|\psi| = D$ in the distribution as L increases [28]. Fig. 3(b) shows the size-dependent anisotropy parameter $\phi_4 = \langle \cos 4\theta \rangle$ for systems at their transition points, with θ extracted from equal-time values of D_x, D_y defined in Eq. (3b). For $SU(2)$ and $SU(3)$, the transition point is determined via the cumulant crossings in Fig. 1(a), while for $SU(4)$ and $SU(5)$ we use the size-dependent point where the energy distribution [Fig. 2] is maximally bimodal. If anisotropy remains, ϕ_4 will converge to a nonzero value, as it does for $N > 2$, while $\phi_4 \rightarrow 0$ if there is emergent $U(1)$ symmetry. In the case of $SU(2)$, we do find emergent $U(1)$ symmetry for the system sizes studied here [presumably also $SO(5)$ but we have not investigated it here]. The size

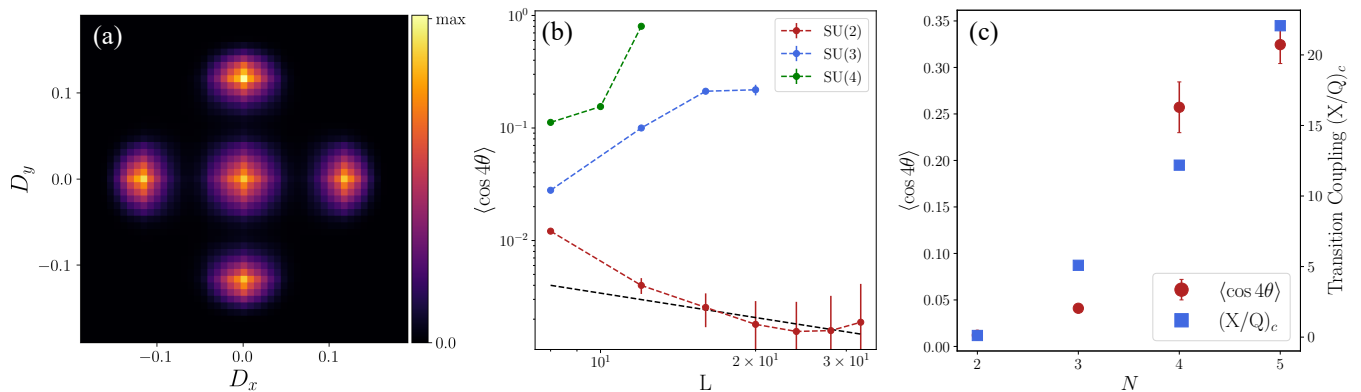


FIG. 3. (a) Distribution of the VBS order parameter $\psi = D_x + iD_y$ at the transition point for the SU(3) $L = 20$ system. Peaks at $(D_x, D_y) = (\pm D, 0), (0, \pm D)$ correspond to the VBS order and the peak at $|D| = 0$ arises from coexistence with the AFM phase. (b) The anisotropy parameter increases with L for SU(3) and SU(4) but decreases for SU(2), with the line indicating the expected $L^{-\mu}$ form with $\mu = 0.72$ [63] for a system sufficiently close to the DQC point. (c) Anisotropy parameter (red, left axis) for $L = 8$ at the estimated $L \rightarrow \infty$ transition points (blue, right axis) for SU(2)-SU(5). Both increase with N .

dependence $\phi_4 \sim L^{-\mu}$ reflects the scaling dimension of the perturbation, which was determined by much more comprehensive results for the J - Q model [63]; $\mu \approx 0.72$. Though the results in Fig. 3(b) are noisy, they are consistent with the same exponent.

In Fig. 3(c) we consider a fixed system size $L = 8$, the largest size that can be equilibrated for SU(5), and plot the transition couplings as well in the same graph. Both the transition coupling $(X/Q)_c$ and the anisotropy ϕ_4 increase with N , demonstrating the correlation between the two.

Discussion.—The X - Q model is not the first to exhibit a strongly first-order AFM-VBS transition. Past studies of SU(2) J - Q type models with the singlet projectors of the Q terms arranged in ways not favoring local singlet fluctuations have been carried out for both square [76] and honeycomb [77] lattices. In those cases, the anisotropy is relevant by construction, and, consequently, the models host conventional strongly first-order transitions with no influence of any nearby critical point. In the X - Q model the emergent U(1) symmetry is violated in a more subtle manner, which we can relate to the way an X term acts on a local 2×2 plaquette with two parallel singlets, illustrated and compared with a Q term in Fig. 4. While the Q term (and the not shown J terms) flips the two singlets, the X term does not. Thus, while a series of Q interactions can gradually flip pairs of singlets, thereby rotating the global VBS order, the X terms do not induce these fluctuations that are necessary for emergent U(1) symmetry and the flow to the CP^{N-1} continuum theory associated with DQC.

For $N \rightarrow \infty$, a columnar VBS pattern is an eigenstate of the Q interaction. This can be easily seen as follows: in the generalized SU(N) valence-bond (singlet) basis, any off-diagonal operation with P operators in Eq. (1) has a matrix element of order $1/N$ [19]. Thus, for $N \rightarrow \infty$

the diagonal interactions dominate and are maximized by the columnar pattern. This, in combination with the absence of U(1) fluctuations from the X term, means the large- N behavior moves closer to the perfect columnar VBS state, in contrast to the SU(N) extended J - Q models where the AFM and VBS inducing interactions compete at the transition even for $N \rightarrow \infty$ [37, 38]. It is then clear that $(X/Q)_c$ is not close to any critical point for large N , and it is then also not appropriate to think of the lattice in this model as perturbing a U(1) DQC point. The higher symmetry is simply not induced by the microscopic interactions in the first place. Apparently, this first-order mechanism is at play in the X - Q model already for $N = 3$, which we observe quantitatively in the fact that the anisotropy ϕ_4 increases with L starting from the smallest systems in Fig. 3(b). In contrast, in the case of $N = 2$, ϕ_4 decreases, following closely a power-law. This indicates that the system with its rather small $(X/Q)_c \approx 0.11$ value (i.e., the Q term with its plaquette flipping property dominates) is near-critical, and the picture of an irrelevant lattice perturbation holds.

The emergent SO(5) symmetry for (only) $N = 2$ [27] is a possible additional contributing factor for this case being special. Given that the Q -only model is already quite close to critical [28], it also has significant SO(5) character. The small X term can then be seen as a weak perturbation of such a critical point, and, while suppressing U(1) fluctuations of the VBS, it may not be a drastic perturbation to the fluctuations between the AFM and VBS sectors.

In both the J - Q and SU(2) X - Q models, in the scenario of Ref. [63], the primary reason for the system not being exactly at the DQC point is not a lack of emergent symmetry (which is a secondary effect) but the presence of an SO(5) singlet perturbation that is not tuned away by only changing a ratio such as J/Q . The multicritical

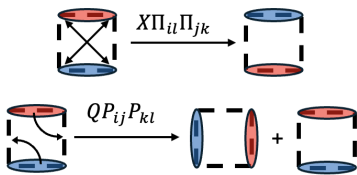


FIG. 4. Action of the X permutation and Q singlet-projector on a single VBS plaquette. The X term swaps singlets but does not mix VBS orientations. The Q term rotates VBS orientations, leading to $U(1)$ resonances. Red/Blue color is only for visual clarity, all singlets are equivalent.

point, which is supported also by CFT work [64], requires additional interactions. However, reaching the singular point without a QMC sign problem may not be possible, or at the very least requires interactions not yet considered. It will certainly be interesting to study a combined J - X - Q model, similar to the J - Q model with higher-order Q terms in Ref. [63]. There the system was tuned from weak to moderately strong first-order transitions, with scaling behavior on the coexistence line consistent with the expectations with the exponents extracted in other ways. The effects of X interactions for both small and large N should give further insights into the nature of perturbed DQC transitions.

Acknowledgements.—This research was supported by the Simons Foundation under Grant No. 511064. The numerical calculations were carried out on the Shared Computing Cluster managed by Boston University’s Research Computing Services.

APPENDIX: $SU(N)$ ALGEBRA

Here we list our choices for the Cartan generators H^a which are used to compute the order parameters m_s^a and D_μ^a in Eq. (3). There are different conventions with which these can be chosen, although no results in this work depend on the convention. For $SU(2)$ there is only one diagonal generator, and the typical choice is

$$H_1 = S^z = \frac{1}{2} \begin{pmatrix} 1 & 0 \\ 0 & -1 \end{pmatrix}$$

For $SU(3)$ we can write the Cartan matrices in terms of the Gell-Mann matrices λ_n , which are also related to the generators of the $SU(3)$ algebra with $T^a = 1/2\lambda_a$,

$$H_1 = \frac{1}{2}\lambda_3 = \frac{1}{2} \begin{pmatrix} 1 & 0 & 0 \\ 0 & -1 & 0 \\ 0 & 0 & 0 \end{pmatrix}$$

and

$$H_2 = \frac{1}{2}\lambda_8 = \frac{1}{2\sqrt{3}} \begin{pmatrix} 1 & 0 & 0 \\ 0 & 1 & 0 \\ 0 & 0 & -2 \end{pmatrix}$$

The generalization to higher $SU(N)$ can be written succinctly following [78], with $m = 1, \dots, N - 1$ elements

$$[H_m]_{ij} = \frac{1}{\sqrt{2m(m+1)}} \times \left(\sum_{k=1}^m \delta_{ik}\delta_{jk} - m\delta_{i,m+1}\delta_{j,m+1} \right).$$

Our order parameters for $SU(N)$ systems are $N - 1$ dimensional vectors, given that there are $N - 1$ Cartan matrices. Therefore to define the Binder cumulant such that $U_2 = 0$ in the disordered state (i.e. where $\langle \mathcal{O}^2 \rangle = 0$ for $\mathcal{O} = M_s$ or ψ), we generalize Binder’s result for a scalar random variable [79] (from a trivial Gaussian integral)

$$\langle \mathcal{O}^4 \rangle = 3\langle \mathcal{O}^2 \rangle^2,$$

to a vector order parameter based on the $N - 1$ Cartan matrices. For an isotropic and zero mean vector, which is satisfied in the disordered phase, a simple calculation gives

$$\langle \mathcal{O}^4 \rangle = \frac{N+1}{N-1} \langle \mathcal{O}^2 \rangle^2,$$

which agrees with the result for $O(n)$ models (see Eq. 77 in Ref. [69]), hence our formula for U_2 in Eq. (4).

* rflynn22@bu.edu

† sandvik@bu.edu

- [1] S. Chakravarty, B. I. Halperin, and D. R. Nelson, Two-dimensional quantum Heisenberg antiferromagnet at low temperatures, *Phys. Rev. B* **39**, 2344 (1989).
- [2] E. Manousakis, The spin- $\frac{1}{2}$ Heisenberg antiferromagnet on a square lattice and its application to the cuprous oxides, *Rev. Mod. Phys.* **63**, 1 (1991).
- [3] A. Auerbach, *Interacting Electrons and Quantum Magnetism*, Graduate Texts in Contemporary Physics (Springer-Verlag, New York, 1994).
- [4] S. Sachdev, Low-dimensional quantum field theories of quantum antiferromagnets, in *Low Dimensional Quantum Field Theories for Condensed Matter Physicists*, edited by Y. Lu, S. Lundqvist, and G. Morandi (World Scientific, Singapore, 1995) pp. 381–432.
- [5] M. Inui, S. Doniach, P. J. Hirschfeld, and A. E. Ruckenstein, Coexistence of antiferromagnetism and superconductivity in a mean-field theory of high- T_c superconductors, *Phys. Rev. B* **37**, 2320 (1988).
- [6] P. W. Anderson, Resonating valence bonds: A new kind of insulator?, *Materials Research Bulletin* **8**, 153 (1973).

- [7] P. W. Anderson, The Resonating Valence Bond State in La_2CuO_4 and Superconductivity, *Science* **235**, 1196 (1987).
- [8] A. V. Chubukov, S. Sachdev, and J. Ye, Theory of two-dimensional quantum Heisenberg antiferromagnets with a nearly critical ground state, *Phys. Rev. B* **49**, 11919 (1994).
- [9] P. A. Lee, N. Nagaosa, and X.-G. Wen, Doping a Mott insulator: Physics of high-temperature superconductivity, *Rev. Mod. Phys.* **78**, 17 (2006).
- [10] S. Sachdev, *Quantum Phase Transitions*, 2nd ed. (Cambridge University Press, Cambridge, 2011).
- [11] D. J. Scalapino, A common thread: The pairing interaction for unconventional superconductors, *Rev. Mod. Phys.* **84**, 1383 (2012).
- [12] J. G. Bednorz and K. A. Müller, Possible high T_c superconductivity in the Ba-La-Cu-O system, *Zeitschrift für Physik B* **64**, 189 (1986).
- [13] F. D. M. Haldane, O(3) Nonlinear σ Model and the Topological Distinction between Integer- and Half-Integer-Spin Antiferromagnets in Two Dimensions, *Phys. Rev. Lett.* **61**, 1029 (1988).
- [14] E. Dagotto and A. Moreo, Phase diagram of the frustrated spin-1/2 Heisenberg antiferromagnet in 2 dimensions, *Phys. Rev. Lett.* **63**, 2148 (1989).
- [15] N. Read and S. Sachdev, Valence-bond and spin-Peierls ground states of low-dimensional quantum antiferromagnets, *Phys. Rev. Lett.* **62**, 1694 (1989).
- [16] N. Read and S. Sachdev, Spin-Peierls, valence-bond solid, and Néel ground states of low-dimensional quantum antiferromagnets, *Phys. Rev. B* **42**, 4568 (1990).
- [17] K. Harada, N. Kawashima, and M. Troyer, Néel and Spin-Peierls Ground States of Two-Dimensional $\text{SU}(N)$ Quantum Antiferromagnets, *Phys. Rev. Lett.* **90**, 117203 (2003).
- [18] S. Sachdev, Quantum magnetism and criticality, *Nature Physics* **4**, 173 (2008).
- [19] K. S. D. Beach, F. Alet, M. Mambrini, and S. Capponi, $\text{SU}(N)$ Heisenberg model on the square lattice: A continuous- N quantum Monte Carlo study, *Phys. Rev. B* **80**, 184401 (2009).
- [20] R. K. Kaul, A. Kolezhuk, M. Levin, S. Sachdev, and T. Senthil, Hole dynamics in an antiferromagnet across a deconfined quantum critical point, *Phys. Rev. B* **75**, 235122 (2007).
- [21] F. F. Assaad, M. Imada, and D. J. Scalapino, Charge and spin structures of a $d_{x^2-y^2}$ superconductor in the proximity of an antiferromagnetic Mott insulator, *Phys. Rev. B* **56**, 15001 (1997).
- [22] A. W. Sandvik, S. Daul, R. R. P. Singh, and D. J. Scalapino, Striped Phase in a Quantum XY Model with Ring Exchange, *Phys. Rev. Lett.* **89**, 247201 (2002).
- [23] O. I. Motrunich and A. Vishwanath, Emergent photons and transitions in the O(3) sigma model with hedgehog suppression, *Phys. Rev. B* **70**, 075104 (2004).
- [24] T. Senthil, A. Vishwanath, L. Balents, S. Sachdev, and M. P. A. Fisher, Deconfined Quantum Critical Points, *Science* **303**, 1490 (2004).
- [25] T. Senthil, L. Balents, S. Sachdev, A. Vishwanath, and M. P. A. Fisher, Quantum criticality beyond the Landau-Ginzburg-Wilson paradigm, *Phys. Rev. B* **70**, 144407 (2004).
- [26] M. Levin and T. Senthil, Deconfined quantum criticality and Néel order via dimer disorder, *Phys. Rev. B* **70**, 220403 (2004).
- [27] T. Senthil and M. P. A. Fisher, Competing orders, nonlinear sigma models, and topological terms in quantum magnets, *Phys. Rev. B* **74**, 064405 (2006).
- [28] A. W. Sandvik, Evidence for Deconfined Quantum Criticality in a Two-Dimensional Heisenberg Model with Four-Spin Interactions, *Phys. Rev. Lett.* **98**, 227202 (2007).
- [29] F.-J. Jiang, M. Nyfeler, S. Chandrasekharan, and U.-J. Wiese, From an antiferromagnet to a valence bond solid: evidence for a first-order phase transition, *Journal of Statistical Mechanics: Theory and Experiment* **2008**, P02009 (2008).
- [30] R. G. Melko and R. K. Kaul, Scaling in the Fan of an Unconventional Quantum Critical Point, *Phys. Rev. Lett.* **100**, 017203 (2008).
- [31] J. Lou, A. W. Sandvik, and N. Kawashima, Antiferromagnetic to valence-bond-solid transitions in two-dimensional $\text{SU}(N)$ Heisenberg models with multispin interactions, *Phys. Rev. B* **80**, 180414 (2009).
- [32] J. Lou, A. W. Sandvik, and L. Balents, Emergence of U(1) Symmetry in the 3D XY Model with Z_q Anisotropy, *Phys. Rev. Lett.* **99**, 207203 (2007).
- [33] T. Okubo, K. Oshikawa, H. Watanabe, and N. Kawashima, Scaling relation for dangerously irrelevant symmetry-breaking fields, *Phys. Rev. B* **91**, 174417 (2015).
- [34] H. Shao, W. Guo, and A. W. Sandvik, Monte Carlo Renormalization Flows in the Space of Relevant and Irrelevant Operators: Application to Three-Dimensional Clock Models, *Phys. Rev. Lett.* **124**, 080602 (2020).
- [35] R. K. Kaul and R. G. Melko, Large- N estimates of universal amplitudes of the \mathbb{CP}^{N-1} theory and comparison with a $S = \frac{1}{2}$ square-lattice model with competing four-spin interactions, *Phys. Rev. B* **78**, 014417 (2008).
- [36] R. K. Kaul, Quantum criticality in $\text{SU}(3)$ and $\text{SU}(4)$ antiferromagnets, *Phys. Rev. B* **84**, 054407 (2011).
- [37] R. K. Kaul and A. W. Sandvik, Lattice Model for the $\text{SU}(N)$ Néel to Valence-Bond Solid Quantum Phase Transition at Large N , *Phys. Rev. Lett.* **108**, 137201 (2012).
- [38] M. S. Block, R. G. Melko, and R. K. Kaul, Fate of \mathbb{CP}^{N-1} Fixed Points with q Monopoles, *Phys. Rev. Lett.* **111**, 137202 (2013).
- [39] E. Dyer, M. Mezei, S. S. Pufu, and S. Sachdev, Scaling dimensions of monopole operators in the \mathbb{CP}^{N_b-1} theory in 2+1 dimensions, *Journal of High Energy Physics* **2015**, 037 (2015), erratum: *JHEP* 03 (2016) 111, doi:10.1007/JHEP03(2016)111.
- [40] A. B. Kuklov, M. Matsumoto, N. V. Prokof'ev, B. V. Svistunov, and M. Troyer, Deconfined Criticality: Generic First-Order Transition in the $\text{SU}(2)$ Symmetry Case, *Phys. Rev. Lett.* **101**, 050405 (2008).
- [41] K. Harada, T. Suzuki, T. Okubo, H. Matsuo, J. Lou, H. Watanabe, S. Todo, and N. Kawashima, Possibility of deconfined criticality in $\text{SU}(N)$ Heisenberg models at small N , *Phys. Rev. B* **88**, 220408 (2013).
- [42] K. Chen, Y. Huang, Y. Deng, A. B. Kuklov, N. V. Prokof'ev, and B. V. Svistunov, Deconfined Criticality Flow in the Heisenberg Model with Ring-Exchange Interactions, *Phys. Rev. Lett.* **110**, 185701 (2013).
- [43] A. Nahum, J. T. Chalker, P. Serna, M. Ortuño, and A. M. Somoza, Deconfined Quantum Criticality, Scaling Violations, and Classical Loop Models, *Phys. Rev. X* **5**, 041048 (2015).

- (2015).
- [44] B. Zhao, J. Takahashi, and A. W. Sandvik, Multicritical Deconfined Quantum Criticality and Lifshitz Point of a Helical Valence-Bond Phase, *Phys. Rev. Lett.* **125**, 257204 (2020).
- [45] J. D’Emidio, A. A. Eberharter, and A. M. Läuchli, Diagnosing weakly first-order phase transitions by coupling to order parameters, *SciPost Phys.* **15**, 061 (2023).
- [46] A. W. Sandvik, Continuous Quantum Phase Transition between an Antiferromagnet and a Valence-Bond Solid in Two Dimensions: Evidence for Logarithmic Corrections to Scaling, *Phys. Rev. Lett.* **104**, 177201 (2010).
- [47] A. Nahum, P. Serna, J. T. Chalker, M. Ortuño, and A. M. Somoza, Emergent SO(5) Symmetry at the Néel to Valence-Bond-Solid Transition, *Phys. Rev. Lett.* **115**, 267203 (2015).
- [48] H. Shao, W. Guo, and A. W. Sandvik, Quantum criticality with two length scales, *Science* **352**, 213 (2016), <https://www.science.org/doi/pdf/10.1126/science.aad5007>.
- [49] R. Ma and C. Wang, Theory of deconfined pseudocriticality, *Phys. Rev. B* **102**, 020407 (2020).
- [50] A. Nahum, Note on Wess-Zumino-Witten models and quasiuniversality in 2 + 1 dimensions, *Phys. Rev. B* **102**, 201116 (2020).
- [51] Z. Zhou, L. Hu, W. Zhu, and Y.-C. He, SO(5) Deconfined Phase Transition under the Fuzzy-Sphere Microscope: Approximate Conformal Symmetry, Pseudo-Criticality, and Operator Spectrum, *Phys. Rev. X* **14**, 021044 (2024).
- [52] S.-S. Gong, W. Zhu, D. N. Sheng, O. I. Motrunich, and M. P. A. Fisher, Plaquette Ordered Phase and Quantum Phase Diagram in the Spin- $\frac{1}{2}$ J_1 - J_2 Square Heisenberg Model, *Phys. Rev. Lett.* **113**, 027201 (2014).
- [53] S. Morita, R. Kaneko, and M. Imada, Quantum Spin Liquid in Spin 1/2 J_1 - J_2 Heisenberg Model on Square Lattice: Many-Variable Variational Monte Carlo Study Combined with Quantum-Number Projections, *Journal of the Physical Society of Japan* **84**, 024720 (2015).
- [54] L. Wang and A. W. Sandvik, Critical Level Crossings and Gapless Spin Liquid in the Square-Lattice Spin-1/2 $J_1 - J_2$ Heisenberg Antiferromagnet, *Phys. Rev. Lett.* **121**, 107202 (2018).
- [55] F. Ferrari and F. Becca, Gapless spin liquid and valence-bond solid in the J_1 - J_2 Heisenberg model on the square lattice: Insights from singlet and triplet excitations, *Phys. Rev. B* **102**, 014417 (2020).
- [56] Y. Nomura and M. Imada, Dirac-Type Nodal Spin Liquid Revealed by Refined Quantum Many-Body Solver Using Neural-Network Wave Function, Correlation Ratio, and Level Spectroscopy, *Phys. Rev. X* **11**, 031034 (2021).
- [57] L. Wang, Y. Zhang, and A. W. Sandvik, Quantum Spin Liquid Phase in the Shastry-Sutherland Model Detected by an Improved Level Spectroscopic Method, *Chinese Physics Letters* **39**, 077502 (2022).
- [58] W.-Y. Liu, J. Hasik, S.-S. Gong, D. Poilblanc, W.-Q. Chen, and Z.-C. Gu, Emergence of Gapless Quantum Spin Liquid from Deconfined Quantum Critical Point, *Phys. Rev. X* **12**, 031039 (2022).
- [59] W.-Y. Liu, D. Poilblanc, S.-S. Gong, W.-Q. Chen, and Z.-C. Gu, Tensor network study of the spin- $\frac{1}{2}$ square-lattice J_1 - J_2 - J_3 model: Incommensurate spiral order, mixed valence-bond solids, and multicritical points, *Phys. Rev. B* **109**, 235116 (2024).
- [60] L. L. Viteritti, R. Rende, A. Parola, S. Goldt, and F. Becca, Transformer wave function for two dimensional frustrated magnets: Emergence of a spin-liquid phase in the Shastry-Sutherland model, *Phys. Rev. B* **111**, 134411 (2025).
- [61] A. Feuerpfel, L. Shackleton, A. Maity, R. Thomale, S. Sachdev, and Y. Iqbal, Unifying dirac spin liquids on square and shastry-sutherland lattices via fermionic deconfined criticality, arXiv preprint arXiv:2601.19980 (2026), arXiv:2601.19980 [cond-mat.str-el].
- [62] L. Shackleton, A. Thomson, and S. Sachdev, Deconfined criticality and a gapless F_2 spin liquid in the square-lattice antiferromagnet, *Phys. Rev. B* **104**, 045110 (2021).
- [63] J. Takahashi, H. Shao, B. Zhao, W. Guo, and A. W. Sandvik, SO(5) multicriticality in two-dimensional quantum magnets (2024), arXiv:2405.06607 [cond-mat.str-el].
- [64] S. M. Chester and N. Su, Bootstrapping deconfined quantum tricriticality, *Phys. Rev. Lett.* **132**, 111601 (2024).
- [65] J. Zhao, Y.-C. Wang, Z. Yan, M. Cheng, and Z. Y. Meng, Scaling of entanglement entropy at deconfined quantum criticality, *Phys. Rev. Lett.* **128**, 010601 (2022).
- [66] J. D’Emidio and A. W. Sandvik, Entanglement Entropy and Deconfined Criticality: Emergent SO(5) Symmetry and Proper Lattice Bipartition, *Phys. Rev. Lett.* **133**, 166702 (2024).
- [67] M. Song, J. Zhao, M. Cheng, C. Xu, M. Scherer, L. Janssen, and Z. Y. Meng, Evolution of entanglement entropy at SU(N) deconfined quantum critical points, *Science Advances* **11**, eadr0634 (2025).
- [68] A. W. Sandvik, Stochastic series expansion method with operator-loop update, *Phys. Rev. B* **59**, R14157 (1999).
- [69] A. W. Sandvik, Computational Studies of Quantum Spin Systems, *AIP Conference Proceedings* **1297**, 135 (2010).
- [70] P. Sengupta, A. W. Sandvik, and D. K. Campbell, Bond-order-wave phase and quantum phase transitions in the one-dimensional extended hubbard model, *Physical Review B* **65**, 155113 (2002).
- [71] K. Hukushima and K. Nemoto, Exchange Monte Carlo Method and Application to Spin Glass Simulations, *Journal of the Physical Society of Japan* **65**, 1604 (1996).
- [72] K. Vollmayr, J. D. Reger, M. Scheucher, and K. Binder, Finite size effects at thermally-driven first order phase transitions: A phenomenological theory of the order parameter distribution, *Zeitschrift für Physik B: Condensed Matter* **91**, 113 (1993).
- [73] S. Iino, S. Morita, N. Kawashima, and A. W. Sandvik, Detecting Signals of Weakly First-order Phase Transitions in Two-dimensional Potts Models, *Journal of the Physical Society of Japan* **88**, 034006 (2019).
- [74] G. J. Sreejith, S. Powell, and A. Nahum, Emergent SO(5) Symmetry at the Columnar Ordering Transition in the Classical Cubic Dimer Model, *Phys. Rev. Lett.* **122**, 080601 (2019).
- [75] J. Takahashi and A. W. Sandvik, Valence-bond solids, vestigial order, and emergent SO(5) symmetry in a two-dimensional quantum magnet, *Phys. Rev. Res.* **2**, 033459 (2020).
- [76] A. Sen and A. W. Sandvik, Example of a first-order Néel to valence-bond-solid transition in two dimensions, *Physical Review B* **82**, 174428 (2010).
- [77] A. Banerjee, K. Damle, and A. Paramekanti, Néel to staggered dimer order transition in a generalized honeycomb lattice Heisenberg model, *Phys. Rev. B* **83**, 134419 (2011).
- [78] H. Georgi, *Lie Algebras in Particle Physics: From Isospin*

to *Unified Theories*, 2nd ed., Frontiers in Physics, Vol. 54
(Perseus Books, Reading, MA, 1999).

[79] K. Binder, Finite size scaling analysis of ising model

block distribution functions, *Zeitschrift fuer Physik B
Condensed Matter* **43**, 119 (1981).